Nanowires

DOI: 10.1002/anie.200601078

Nanocrystal-Mediated Crystallization of Silicon and Germanium Nanowires in Organic Solvents: The Role of Catalysis and Solid-Phase Seeding**

*Hsing-Yu Tuan, Doh C. Lee, and Brian A. Korgel**

The size-dependent properties, large surface-area-to-volume ratios, dispersibility in solvents, and mechanical flexibility of semiconductor nanowires make them an exciting class of materials.[1–3] Silicon nanowires in particular can be both *n* and *p*-doped and interface well with an insulating oxide and conducting metal silicide and these nanowires might be applied in silicon CMOS (complementary metal oxide semiconductor) circuits or with organic compounds on flexible plastic substrates.[4,5] Germanium is similar to silicon in many respects, but with a higher carrier mobility. Gold-seeded vapor–liquid–solid (VLS) growth is a common route to silicon and germanium nanowire synthesis at low growth temperatures ($\approx$360 °C).[1,3,6–8] Unfortunately, gold traps electrons and holes in both silicon and germanium and poses a serious contamination problem for nanowire integration with silicon CMOSs. Surprisingly few gold alternatives have been investigated for nanowire seeding. Si nanowires have been seeded by chemical vapor deposition (CVD) with Ti particles[9] and Ga droplets,[10] and in organic solvents, Si and Ge nanowires were synthesized using Ni nanocrystals.[11,12] Gold alternatives have been explored more extensively for other semiconductors: Sn for ZnO wires,[13] various metal films for vapor-grown tin oxide nanowires,[14] and low-melting metals such as In and Bi for solution synthesis of Group II–VI,[15,16] III-V[17–19] and Ge nanowires.[20] Herein, many different nanocrystals—Co, Ni, CuS, Mn, Ir, $MnPt_3$, Fe_2O_3, and FePt—are explored as seeds for Si and Ge nanowire synthesis to develop a more general understanding of the role of the seed particles in the nanowire growth process.

Si and Ge nanowires were grown by decomposing silanes or germanes in high temperature (450–500 °C), high pressure (10.3 MPa) supercritical toluene.[21,22] Under these reaction conditions, Au nanocrystals seed nanowires by the "supercritical fluid–liquid–solid" (SFLS) mechanism in which nanowires evolve from a liquid Au:Si (or Au:Ge) eutectic. In combination with Si and Ge, many of the seed materials studied herein do not form liquid eutectics until reaching temperatures well above 500 °C, and are not expected to work for "VLS"-like growth. However, they form solid alloys below 500 °C, perhaps making solid-phase nanowire seeding possible. Figure 1 shows TEM images of the various colloidal nanocrystals used to seed Si and Ge nanowires; their size distributions had standard deviations less than 20% about mean diameters ranging between 4.2 and 10.2 nm. Figure 2 shows the reaction products. All of the nanocrystals seeded Si and Ge nanowires from monophenylsilane (MPS) and diphenylgermane (DPG), but with varying success (summar-

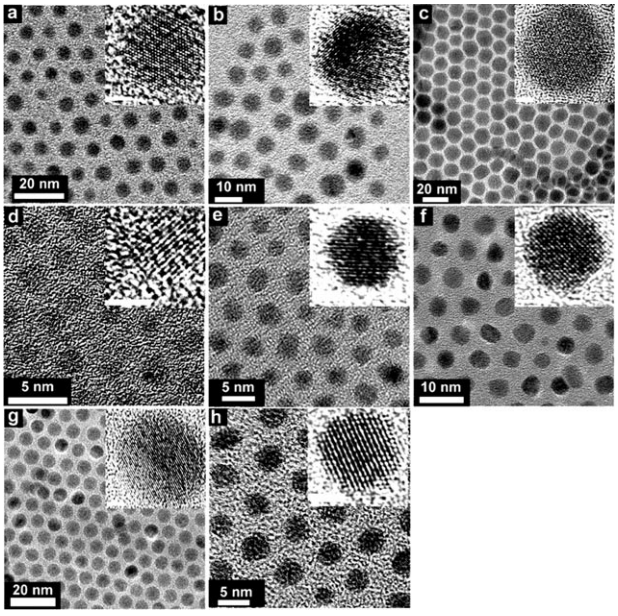

Figure 1. TEM images of metal nanocrystals studied as Si and Ge nanowire seeds: a) Co, b) Ni, c) CuS, d) Mn, e) Ir, f) $MnPt_3$, g) Fe_2O_3 and h) FePt. Insets: magnified images, scale bars 2 nm.

[*] H.-Y. Tuan, D. C. Lee, Prof. B. A. Korgel
Department of Chemical Engineering
Texas Materials Institute
Center for Nano- and Molecular Science and Technology
The University of Texas
Austin, TX 78712-1062 (USA)
Fax: (+1) 512-471-7060
E-mail: korgel@mail.che.utexas.edu

[**] We acknowledge the National Science Foundation, the Robert A. Welch Foundation, the Advanced Materials Research Center in collaboration with International SEMATECH, the Advanced Processing and Prototyping Center (DARPA: HR0011-06-1-0005), and the Office of Naval Research (N00014-05-1-0857) for financial support of this research. We are grateful to Felice Shieh, Cindy Stowell, and Ali Ghezelbash for Co, Ir, and CuS nanocrystals, and to J. P. Zhou for TEM assistance.

Supporting information for this article is available on the WWW under http://www.angewandte.org or from the author.

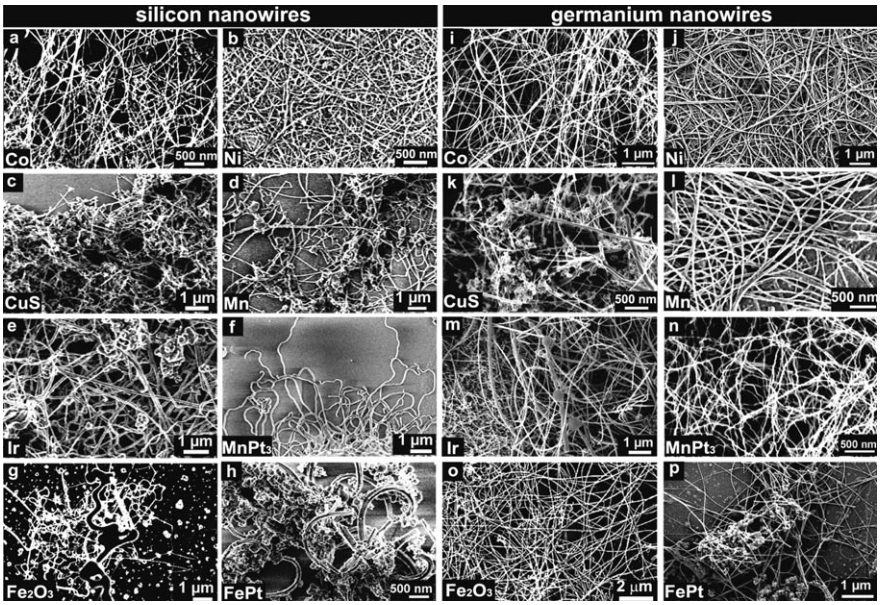

Figure 2. SEM images of a–h) Si and i–p) Ge nanowires synthesized in supercritical toluene from MPS (150 mM, 500 °C, 10.3 MPa) and DPG (80 mM, 460 °C, 10.3 MPa), respectively.

ized in Table 1). In general, straight nanowires are crystalline with few extended defects, whereas curly wires are usually amorphous or polycrystalline.[23] Co nanocrystals gave the highest yield of straight, long (> 10 μm) Si and Ge nanowires (Figure 3). Ni nanocrystals also produced crystalline Si and Ge nanowires with good yield. CuS nanocrystals produced straight crystalline Si nanowires with good yield but slightly shorter lengths (3–10 μm) and Fe_2O_3 nanocrystals produced high quality Ge nanowires with relatively high yield.

All of the nanocrystals produced nanowires at temperatures significantly below their bulk eutectic temperatures (summarized in Table 1). The small size of the seed nanocrystals reduces the eutectic temperature; however, a drop of nearly 350 °C is unlikely.[12] These nanocrystals most likely promote nanowire crystallization from solid-phase seeds. Solid-phase metal-seeded nanowire growth has also been proposed in other systems: Si (Ti,[9] Ni[11]), Ge (Fe,[24] Ni[12]), GaAs (Au),[25] InAs (Au),[26] and ZnSe (Au,[27] Fe[28]) nanowires. Solid-phase seeding is a viable growth mechanism, provided that the seed particles are small enough for rapid saturation by solid-state diffusion and the semiconductor has a high solid solubility in the metal. Co, Ni, Fe, and Cu all form alloys with Si and Ge at the growth temperatures and energy dispersive spectroscopy (EDS) analysis of the seed particles found at the tips of many nanowires revealed silicide and germanides (see Supporting Information for representative data). In the particles located at the tips of nanowires seeded with CuS and Fe_2O_3 nanocrystals, S and O were not observed in significant quantities, indicating that wires probably crystallize from copper silicide and iron germanide phases. Perhaps CuS and Fe_2O_3 are first reduced to Cu and Fe metal in the reaction mixture, prior to nanowire growth. Particles found at the tips of FePt-seeded nanowires showed all three elements—Fe, Pt, and Ge—indicating that nanowire growth probably originates from a ternary Fe:Pt:Ge phase.

Si and Ge nanowires seeded with Ni, Co, Fe_2O_3, and CuS show two predominant growth directions—⟨111⟩ and ⟨110⟩—in nearly equal proportions (Figure 3). Approximately 5% of the nanowires also had ⟨112⟩-oriented growth. This result is different from that for Au-seeded Si and Ge nanowires in organic solvents, which show preferential growth in either the ⟨111⟩ (Si) or ⟨110⟩ (Ge) directions, with only a small proportion of ⟨110⟩ (or ⟨111⟩) and ⟨112⟩ orientations.[22,29] Perhaps the difference in nanowire growth direction relates to the solid-phase

Table 1: Summary of seed nanocrystal composition and selected properties and reaction conditions.

Nanowire	Seed	Nanocrystal diameter [nm]	Reaction temp. [°C][a]	Eutectic temp. [°C][h]	Product description
Si	Co	9.7	500[b]	1200	Long straight wires
Si	Ni	5.6	460	964	Long straight wires
Si	CuS	11.7	500	802[d]	Good yield, shorter wires
Si	Mn	4.7	500	1040	Crystalline wires, low yield
Si	Ir	4.2	500	1470	Amorphous particles & curly wires
Si	$MnPt_3$	5.1	500	N/A	Low yield, mostly curly wires
Si	Fe_2O_3	10.2	500	1200[e]	Amorphous particles & few wires
Si	FePt	4.3	500	N/A	Amorphous particles
Ge	Co	9.7	460[c]	817	Long straight wires
Ge	Ni	5.6	460	762	Long straight wires
Ge	CuS	11.7	460	644[f]	Short curly wires
Ge	Mn	4.7	460	720	Crystalline wires, low yield
Ge	Ir	4.2	460	N/A	Wires & amorphous particles
Ge	$MnPt_3$	5.1	460	N/A	Straight wires with rough surfaces
Ge	Fe_2O_3	10.2	460	838[g]	Long straight wires
Ge	FePt	4.3	460	N/A	Wires & amorphous particles

[a] The optimal synthesis temperature for Si nanowires was approximately 40 °C higher than for Ge nanowires in all cases, indicating slower Si nanowire growth kinetics. [b] The optimum reaction temperature for cobalt-seeded Si nanowires from MPS was approximately 50 °C higher than the optimal synthesis temperature (450 °C) using Au seeds. [c] The optimum reaction temperature for cobalt-seeded Ge nanowires from DPG is approximately 80 °C higher than the optimal synthesis temperature (380 °C) using Au seeds. [d] Value based on Cu:Si phase diagram, because S appears to outgas from the seed particles. [e] Value based on Fe:Si phase diagram, because iron silicide appears to be the seed composition. [f] Value based on Cu:Ge phase diagram, because S appears to outgas from the seed particles. [g] Value based on Fe:Ge phase diagram, because iron germanocide appears to be the seed composition. [h] Ref. [42].

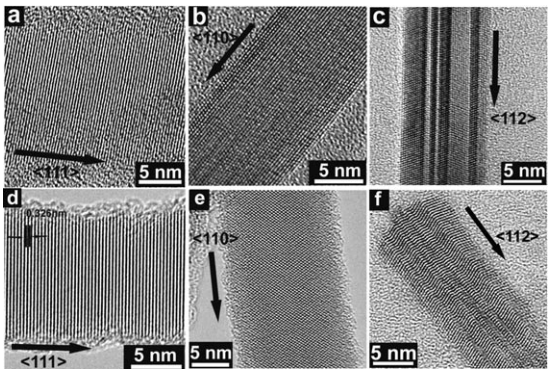

Figure 3. HRTEM images of Si (a–c) and Ge (d–f) nanowires seeded by Co (a–c), Fe_2O_3 (d–e), and CuS (f) showing ⟨110⟩, ⟨111⟩ and ⟨112⟩ growth directions. Approximately 5% of the sample contained ⟨112⟩ oriented nanowires, usually with longitudinal {111} twins, as in (c) and (f). The 0.326 nm lattice spacing agrees with the (111) d-spacing for bulk Ge (0.327 nm).

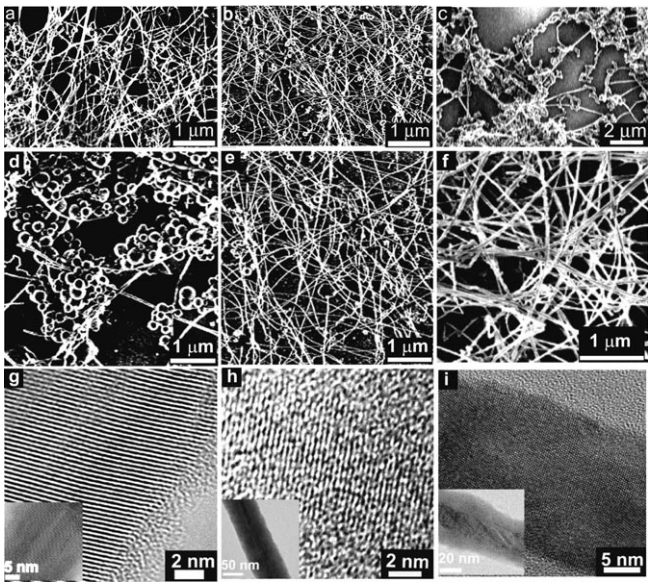

Figure 4. Cobalt-nanocrystal-seeded Si nanowires. HRSEM images of Si nanowires synthesized in supercritical toluene (10.3 MPa) from a) MPS (500 °C), b) trisilane (400 °C), and c) octylsilane (500 °C). HRSEM images of Si nanowires synthesized in supercritical toluene (10.3 MPa) from trisilane at d) 350 °C, e) 400 °C, and f) 450 °C. g–i) TEM images of Si nanowires synthesized in supercritical toluene (10.3 MPa) with g) trisilane (400 °C), h) trisilane (450 °C) and i) octylsilane (500 °C). The nanowires in (h) and (i) are coated with an amorphous shell, as shown more clearly in the low-resolution TEM images in the insets in (h) and (i). The shell material in (h) is amorphous Si and in (i) it is amorphous 3:1 C:Si (by EDS).

nanowire seeding process. However, it is noteworthy that regardless of the metal used to seed the nanowires (i.e., Au, Ni, or Co.), ⟨112⟩-oriented nanowires always tend to have longitudinal {111} twins, as in the wires in Figure 3c and f.

In VLS growth, the metal seed dissolves the semiconductor and recrystallizes it as a nanowire and has a passive role in the precursor decomposition chemistry.[3,6,22] Au does not catalyze reactant decomposition, but simply helps drive crystallization (Au could be called a "crystallization catalyst", but not a catalyst for reactant decomposition). In contrast to Au, the transition metals Ni, Co, and Fe, are catalysts for molecular decomposition reactions. For carbon nanotube (CNT) growth, Fe, Co, and Ni are used as catalysts that enhance reactant decomposition at the seed surface, while also promoting "crystallization" of the nanostructure—for CNTs that is graphitization and tube growth.[30–32] Au-seeded CVD nanowire growth typically uses very reactive precursors, such as silane, and there is generally no need to use catalytic seed metals to promote reactant decomposition. However, sidewall deposition can occur with reactive precursors and lead to substantial diameter tapering over the length of the wire.[33,34] Catalytic seeds might be able to lower the growth temperature and help prevent sidewall deposition. In Au-seeded, solution-phase nanowire growth, many organosilane and organogermane reactants, such as octylsilane, are too unreactive to promote nanowire formation at typical reaction temperatures.[11,22] Trisilane on the other hand is too reactive and forms amorphous Si particles.[22] These Si reactants require a catalytic seed to promote nanowire formation.

Figure 4 shows TEM and SEM images of Si nanowires seeded by Co nanocrystals in supercritical toluene from MPS, trisilane, and octylsilane—all three reactants gave nanowires. The cobalt nanocrystals enhance octylsilane decomposition enough to promote nanowire formation; however, the nanowire quality is only marginal as the nanowires are coated with an amorphous layer with significant carbon content (Figure 4i, 3:1 C:Si by EDS in shell). The cobalt nanocrystals were found to promote Si nanowire formation using trisilane at temperatures as low as 350 °C, although the majority product at this low temperature was amorphous Si colloids (Figure 4d). Cobalt enhances heterogeneous trisilane decomposition relative to homogeneous particle formation. Si nanowires produced with trisilane at 400 °C had very little sidewall deposition and few particulates; slightly higher temperature (450 °C) gave significant sidewall deposition (Figure 4h).

Of the nanocrystals studied, Co gave the highest yield and quality of both Si and Ge nanowires, rivaling Au-seeded reactions (See Supporting Information for an example of Au-seeded Si nanowires). All growth temperatures were well below the bulk eutectic temperatures, indicating solid-phase seeding. Solid-phase seeding can probably occur for any semiconductor with a high solubility in the seed metal; however, the growth temperature must be sufficiently high for fast saturation by solid-state diffusion, which can occur relatively fast in nanometer-diameter seed particles. Cobalt was also found to catalyze silane decomposition to promote Si nanowire growth from octylsilane and trisilane, similar to past studies on Ni nanocrystals.[11,12] In gas-phase reactions, the use of catalytic transition-metal seeds might enable lower temperature reactions for less sidewall deposition and better diameter control. As more seed materials are studied, the solid-phase growth method may become as prevalent as liquid-eutectic seeding, and the use of catalytic seed particles might serve as a general approach for improved diameter control, as it has for carbon nanotube growth.

Experimental Section

Anhydrous toluene (99.8%, Sigma-Aldrich), monophenylsilane (MPS, 97%, Sigma-Aldrich), *N*-octylsilane ($(C_8H_{17})H_3Si$, Gelest), trisilane (Si_3H_8, Voltaix), and diphenylgermane (DPG, Gelest) were used as received. Co,[35] Ni,[36] CuS,[37] Ir,[38] Mn (Supporting Information), $MnPt_3$, Fe_2O_3,[39] and FePt[40] nanocrystals were prepared by arrested precipitation as described in the literature.

Nanowires were synthesized in semibatch 1 mL or 10 mL Ti grade-2 reactor connected to a high-pressure liquid chromatography (HPLC) pump for pressure control and reactant injection. The reactor was heated in a brass block with temperature monitored by a thermocouple.[22,32,41] A small piece of clean Si wafer was placed in the reactor as a deposition substrate to gather reaction product. The reactor was sealed in a nitrogen-filled glove box, connected to the HPLC pump, and then filled with anhydrous oxygen-free toluene. The reactor was pressurized to 3.4 MPa with toluene and then heated to the reaction temperature. 500 μL of 150 mM MPS in toluene with Si:nanocrystal mole ratios of 50:1 (Co), 100:1 (Ni), 150:1 (CuS), 50:1 (Mn), 50:1 (Ir), 50:1 ($MnPt_3$), 50:1 (Fe_2O_3), and 50:1 (FePt), were injected from a six-way valve injection loop (Valco) at 0.4 mL min^{-1}. For Ge nanowires, 500 μL of 80 mM DPG in toluene were injected with Ge:nanocrystal mole ratios of 100:1 (Co), 100:1 (Ni), 100:1 (CuS), 50:1 (Mn), 20:1 (Ir), 100:1 ($MnPt_3$), 200:1 (Fe_2O_3), and 200:1 (FePt). The reaction pressure was increased to 10.3 MPa with additional toluene. After 10 min, the reactor was immersed in ice-water and cooled to room temperature. The reactor was opened and the deposition substrate removed and stored under nitrogen until the product was characterized by SEM and TEM.

Nanowires were imaged by HRSEM on the deposition substrate without further purification using a LEO 1530 field-emission SEM at 1–3 kV accelerating voltage with working distances ranging between 2–5 mm. For HRTEM and STEM imaging, nanowires were either drop-cast from chloroform dispersions or dry transferred by scratching the deposition substrate onto 200-mesh lacey carbon-coated copper or nickel grids (Electron Microscope Sciences). Images were acquired using 200 kV accelerating voltage on a JEOL 2010F equipped with an Oxford INCA ED spectrometer.

Received: March 20, 2006
Revised: May 1, 2006
Published online: July 5, 2006

Keywords: germanium · nanocrystals · nanowires · silicon · supercritical fluids

[1] J. D. Holmes, K. P. Johnston, R. C. Doty, B. A. Korgel, *Science* **2000**, *287*, 1471.
[2] B. A. Korgel, *Science* **2004**, *303*, 1308.
[3] For a recent review, see M. Law, J. Goldberger, P. Yang, *Annu. Rev. Mater. Res.* **2004**, *34*, 83.
[4] Y. Cui, C. M. Lieber, *Science* **2001**, *291*, 851.
[5] M. C. McAlpine, R. S. Friedman, S. Jin, K. H. Lin, W. U. Wang, C. M. Lieber, *Nano Lett.* **2003**, *3*, 1531.
[6] J. T. Hu, T. W. Odom, C. M. Lieber, *Acc. Chem. Res.* **1999**, *32*, 435.
[7] T. Hanrath, B. A. Korgel, *Adv. Mater.* **2003**, *15*, 437.
[8] D. W. Wang, H. J. Dai, *Angew. Chem.* **2002**, *114*, 4783; *Angew. Chem. Int. Ed.* **2002**, *41*, 4783.
[9] T. I. Kamins, R. S. Williams, D. P. Basile, T. Hesjedal, J. S. Harris, *J. Appl. Phys.* **2001**, *89*, 1008.
[10] M. K. Sunkara, S. Sharma, R. Miranda, G. Lian, E. C. Dickey, *Appl. Phys. Lett.* **2001**, *79*, 1546.
[11] H.-Y. Tuan, D. C. Lee, T. Hanrath, B. A. Korgel, *Nano Lett.* **2005**, *5*, 681.
[12] H.-Y. Tuan, D. C. Lee, T. Hanrath, B. A. Korgel, *Chem. Mater.* **2005**, *17*, 5705.
[13] Y. Ding, P. X. Gao, Z. L. Wang, *J. Am. Chem. Soc.* **2004**, *126*, 2066.
[14] P. Nguyen, H. T. Ng, M. Meyyappan, *Adv. Mater.* **2005**, *17*, 1773.
[15] H. Yu, J. B. Li, R. A. Loomis, P. C. Gibbons, L. W. Wang, W. E. Buhro, *J. Am. Chem. Soc.* **2003**, *125*, 16168.
[16] J. W. Grebinski, K. L. Hull, J. Zhang, T. H. Kosel, M. Kuno, *Chem. Mater.* **2004**, *16*, 5260.
[17] T. J. Trentler, K. M. Hickman, S. C. Goel, A. M. Viano, P. C. Gibbons, W. E. Buhro, *Science* **1995**, *270*, 1791.
[18] S. P. Ahrenkiel, O. I. Micic, A. Miedaner, C. J. Curtis, J. M. Nedeljkovic, A. J. Nozik, *Nano Lett.* **2003**, *3*, 833.
[19] D. D. Fanfair, B. A. Korgel, *Cryst. Growth Des.* **2005**, *5*, 1971.
[20] X. Lu, D. D. Fanfair, K. P. Johnston, B. A. Korgel, *J. Am. Chem. Soc.* **2005**, *127*, 15718.
[21] For a recent review, see P. S. Shah, T. Hanrath, K. P. Johnston, B. A. Korgel, *J. Phys. Chem. B* **2004**, *108*, 9574.
[22] D. C. Lee, T. Hanrath, B. A. Korgel, *Angew. Chem.* **2005**, *117*, 3639; *Angew. Chem. Int. Ed.* **2005**, *44*, 3573.
[23] X. Lu, T. Hanrath, K. P. Johnston, B. A. Korgel, *Nano Lett.* **2003**, *3*, 93.
[24] S. Mathur, H. Shen, V. Sivakov, U. Werner, *Chem. Mater.* **2004**, *16*, 2449.
[25] A. I. Persson, M. W. Larsson, S. Stenstroem, B. J. Ohlsson, L. Samuelson, L. R. Wallenberg, *Nature Mater.* **2004**, *3*, 677.
[26] K. A. Dick, K. Deppert, T. Mrtensson, B. Mandl, L. Samuelson, W. Seifert, *Nano Lett.* **2005**, *5*, 761.
[27] Y. Ohno, T. Shirahama, S. Takeda, A. Ishizumi, Y. Kanemitsu, *Appl. Phys. Lett.* **2005**, *87*, 043105.
[28] A. Colli, S. Hofmann, A. C. Ferrari, C. Ducati, F. Martelli, S. Rubini, S. Cabrini, A. Franciosi, J. Robertson, *Appl. Phys. Lett.* **2005**, *86*, 153103.
[29] T. Hanrath, B. A. Korgel, *Small* **2005**, *1*, 717.
[30] H. J. Dai, J. Kong, C. W. Zhou, N. Franklin, T. Tombler, A. Cassell, S. S. Fan, M. Chapline, *J. Phys. Chem. B* **1999**, *103*, 11246.
[31] D. C. Lee, F. V. Mikulec, B. A. Korgel, *J. Am. Chem. Soc.* **2004**, *126*, 4951.
[32] D. C. Lee, B. A. Korgel, *Mol. Simul.* **2005**, *31*, 637.
[33] H. Adhikari, A. F. Marshall, C. E. D. Chidsey, P. C. McIntyre, *Nano Lett.* **2006**, *6*, 318.
[34] E. Tutuc, S. Guha, J. O. Chu, *Appl. Phys. Lett.* **2006**, *88*, 043113.
[35] V. F. Puntes, D. Zanchet, C. K. Erdonmez, A. P. Alivisatos, *J. Am. Chem. Soc.* **2002**, *124*, 12874.
[36] C. B. Murray, S. Sun, H. Doyle, T. Betley, *MRS Bull.* **2001**, *26*, 985.
[37] A. Ghezelbash, B. A. Korgel, *Langmuir* **2005**, *21*, 9451.
[38] C. A. Stowell, B. A. Korgel, *Nano Lett.* **2005**, *5*, 1203.
[39] T. Hyeon, S. S. Lee, J. Park, Y. Chung, H. B. Na, *J. Am. Chem. Soc.* **2001**, *123*, 12798.
[40] S. Sun, C. B. Murray, D. Weller, L. Folks, A. Moser, *Science* **2000**, *287*, 1989.
[41] T. Hanrath, B. A. Korgel, *J. Am. Chem. Soc.* **2002**, *124*, 1424.
[42] *Binary Alloy Phase Diagrams*, 2nd Ed. (Eds.: B. M. Thaddeus, O. Hiroaki, P. R. Subramanian, K. Linda), ASM International, Materials Park, OH, **1990**.

